



# Investigating the impact of edge weight selection on the pig trade network topology

Gavrila A. Puspitarani<sup>a,b</sup>, Yan-Shin Jackson Liao<sup>c,1</sup>, Reinhard Fuchs<sup>d,e</sup>,  
Amélie Desvars-Larrive<sup>a,b</sup>

<sup>a</sup> Unit of Veterinary Public Health and Epidemiology, University of Veterinary Medicine Vienna, Veterinärplatz 1, Vienna, 1210, Vienna, Austria

<sup>b</sup> Complexity Science Hub, Metternichgasse 8, Vienna, 1030, Vienna, Austria

<sup>c</sup> Department of Health and Mental Hygiene, Public Health Laboratory, NY, United States

<sup>d</sup> Department for Data, Statistics and Risk Assessment, Austrian Agency for Health and Food Safety (AGES), Beethovenstraße 6, Graz, 8010, Styria, Austria

<sup>e</sup> Institute of Systems Sciences, Innovation and Sustainability Research, University of Graz, Meranstraße 18, Graz, 8010, Styria, Austria

## ARTICLE INFO

Dataset link: <https://doi.org/10.6084/m9.figsh.26494786.v1>

### Keywords:

Pig trade network  
Weighted network  
Centrality metrics  
Epidemic model

## ABSTRACT

Traceability of animal movements and robust surveillance are crucial for prevention and control of animal diseases. While network analysis has emerged as a powerful tool for identifying higher-risk holdings through centrality metrics, its effectiveness depends on two methodological choices: (1) edge-weighting schemes (movement frequency vs. animal volume) and (2) centrality metric selection. This study investigates how alternative edge-weighting approaches (frequency vs. volume) influence network topology and node centrality rankings in a pig movement network.

Using 2021 pig movement data from Upper Austria (5,766 holdings; 92,914 movements), we: (1) quantify how edge-weighting schemes (frequency vs. volume) affect network topology and community structure, and (2) evaluate node ranking robustness across three centrality metrics (strength, betweenness, closeness) against epidemic simulation rankings. Our analysis reveals distinct edge weight distributions: frequency-based network exhibited a bimodal pattern, while volume-based was more uniform. We observed strong positive correlations ( $\tau > 0.42$ – $0.84$ ;  $p < 0.001$ ) in node rankings across all centrality metrics (strength, closeness, betweenness), with consistent patterns observed both: (i) between frequency- and volume-weighted networks, and (ii) within each network representation. Strength centrality exhibited the highest correlation with the simulation-based rankings, particularly for the top 5% highest-ranked nodes ( $\tau_b = 0.51$  for frequency-based and  $\tau_b = 0.5$  for volume-based). These findings highlight that strength centrality provides a computationally efficient and field-practical alternative to epidemic simulations for identifying high-risk holdings. This enables resource-efficient, data-driven surveillance while maintaining epidemiological relevance.

## 1. Introduction

The transmission dynamic of infectious diseases depends fundamentally on contact patterns between individuals (Keeling and Rohani, 2011). While network models typically simplify these interactions by treating them as binary (i.e. either present or absent) (Newman, 2004), this oversimplification overlooks critical variations in contact rates. Such oversight is epidemiologically significant, as it fails to recognize that some individuals interact more intensely than others and therefore disproportionately drive infectious disease spread (Büttner and Krieter, 2021).

The intensity of the interactions is typically represented as edge weights in network models (Büttner and Krieter, 2021). To realistically represent the contagion process and estimate epidemic metrics, models must therefore move beyond binary consideration within homogeneous-mixing models to incorporate weighted interactions. This requires examining both contact frequency distribution and interaction characteristics between pairs of individuals (Jolly, 2001; Lockhart et al., 1996). In frequency-dependent disease transmission, the contact rate (and therefore the likelihood of transmission of the disease) is

\* Corresponding author at: Unit of Veterinary Public Health and Epidemiology, University of Veterinary Medicine Vienna, Veterinärplatz 1, Vienna, 1210, Vienna, Austria.

E-mail addresses: [gavrila.puspitarani@vetmeduni.ac.at](mailto:gavrila.puspitarani@vetmeduni.ac.at) (G.A. Puspitarani), [yanshinliao@gmail.com](mailto:yanshinliao@gmail.com) (Y.-S.J. Liao), [reinhard.fuchs@ages.at](mailto:reinhard.fuchs@ages.at) (R. Fuchs), [amelie.desvars@vetmeduni.ac.at](mailto:amelie.desvars@vetmeduni.ac.at) (A. Desvars-Larrive).

<sup>1</sup> These authors contributed equally to this work.

<https://doi.org/10.1016/j.epidem.2025.100849>

Received 15 October 2024; Received in revised form 28 May 2025; Accepted 4 August 2025

Available online 22 August 2025

1755-4365/© 2025 The Authors. Published by Elsevier B.V. This is an open access article under the CC BY license (<http://creativecommons.org/licenses/by/4.0/>).

independent of the population size or density. In contrast, in density-dependent disease transmission, contact rates between individuals increase as the population density rises, leading to a subsequent increase in disease transmission (Begon et al., 2002; McCallum, 2001; Keeling and Rohani, 2011). For example, in sexual contact networks, disease transmission risk depends on the number of partners (node degree) and on the coital frequency (edge weights), but is not dependent on the population density. Consequently, weighting contacts is essential to accurately capture heterogeneity in individual contacts and model its impact on disease transmission dynamics (Kamp et al., 2013).

Mobility datasets allow flexible edge weighting to quantify relationship intensity or capacity between network entities (Barrat et al., 2004). In livestock trade networks, edge weights typically represent either trade frequency, i.e., the number of transactions (hereafter referred to as “frequency-based”), or traded volume, i.e., the number of traded animals (“volume-based”) between holdings. These measures can be further aggregated across various time intervals (e.g., daily, monthly, or the entire observation period).

While weighted networks are increasingly used in veterinary epidemiology for analyzing livestock trade data, e.g., in the USA (Pasafaro et al., 2020), Germany (Lentz et al., 2016), and North Macedonia (O’Hara et al., 2022), identify high-risk holdings (Büttner and Krieter, 2018; Candeloro et al., 2016; Natale et al., 2009), and modeling disease transmission (Schley et al., 2012). However, several critical challenges persist in applying these methods for epidemic control. First, while studies have evaluated node importance using either centrality measures (Lentz et al., 2016; Volkova et al., 2010b) or simulation approaches (Schley et al., 2012; Büttner and Krieter, 2021), the field lacks a reproducible framework for node ranking due to inherent heterogeneity in livestock mobility networks and a notable absence of direct comparisons between centrality-based and simulation-based rankings. This limitation is compounded by the fact that current node ranking methods often prioritize technical measures over empirical validation of a node’s actual influence during an epidemic process. While studies have demonstrated the existence of superspreaders in specific networks, these findings demonstrate limited generalizability across diverse real-world scenarios (Chin and Bouffanais, 2020; da Silva et al., 2012; Kitsak et al., 2010). Furthermore, no consensus exists regarding the optimal node centrality measure for quantifying epidemic importance, as metric performance appears highly dependent on both network structure and epidemiological context.

Additionally, the network structure significantly impacts disease transmission. For instance, real-world networks exhibit heterogeneous connectivity patterns across nodes (called degree centrality distribution), where most nodes have few connections while a few act as highly connected hubs (Albert et al., 1999; Büttner et al., 2013; Lentz et al., 2016; Rautureau et al., 2012), which may serve as sentinels for disease surveillance (Bellingeri et al., 2023; Bucur and Holme, 2020). Although Büttner et al. Büttner and Krieter (2021) demonstrated that the type of edge weights affects epidemic size, they did not examine whether high-risk nodes, critical for targeted surveillance, remain consistent across weighting approaches. Moreover, few studies have systematically examined whether different weighting approaches consistently identify influential nodes for surveillance (Trostle et al., 2022; Candeloro et al., 2016). This unresolved methodological question represents a fundamental methodological challenge in network-based risk assessment, with direct consequences for (i) disease control efficacy, as inconsistent node rankings may lead to misallocated surveillance resources; (ii) policy standardization, as current weighting scheme selection lack evidence-based guidelines; and (iii) model reliability, as potential divergence in risk predictions depending on methodological choices.

Collectively, these gaps highlight the need for systematic comparisons of node ranking approaches and their relationship with actual epidemic outcomes across diverse network types.

In this study, we first aimed to explore, from a veterinary epidemiology perspective, whether the selection of edge weights impacts both the topology of an animal trade network and node ranking based on weighted centrality metrics. Our second objective was to address the limited validation of technical network metrics against epidemiological relevance by evaluating whether node rankings from centrality metrics aligned with rankings based on a simulation-based contagion process, used as a benchmark. To achieve these objectives, we analyzed daily pig movement records from Upper Austria in 2021 using methods from social network analysis (Bellingeri et al., 2023). We constructed a weighted directed network, where nodes represented pig holdings and edges represented trade movements. We created two representations of this network to compare two weighting approaches: in the “frequency-based” network, edge weights represented the number of trades between holdings, while in the “volume-based” network, weights reflected the number of animals traded.

We investigated the federal state of Upper Austria (1.53 million inhabitants, 11,982.67 km<sup>2</sup> (Statistics Austria, 2024)) because it contributes 41.7% to the total pig production in the country, exhibits the highest density of pig farms in Austria, and its network of pig movements is more densely connected than in the rest of the country (Puspitarani et al., 2023b). These characteristics create an interesting opportunity for testing surveillance and control strategies that may not be readily applicable to regions with a sparser network. By leveraging a real-world network, our goal was to generate insights that closely mirror field conditions and support practical applications in disease surveillance and prevention within the swine industry.

## 2. Materials and methods

### Data

The Verbrauchergesundheitsinformationssystem (VIS) (Statistics Austria) is a national database that records information on livestock movements and farms in Austria. Each pig movement entry includes the date of the movement (dd.mm.yyyy), the number of animals moved (batch size), the type of movement (e.g., *domestic*, *slaughter*, *abroad*, and *abroad-slaughter*), as well as the source and destination holding (see Puspitarani et al. (2023b,a) for more details). Each holding is identified via a unique anonymized identifier (ID) and associated data includes the number of animals per production stage, randomized 5 km-radius geocoordinates (i.e., latitude and longitude, projected coordinate system EPSG 31287), and the federal state where the holding was located (Upper Austria). Additionally, each holding is labeled according to its type of activity, as self-reported annually by the owner. There are eight possible labels: abattoir, boar station, collection point, cutting plant, farm, private owner, processing plant, and trade and logistics. For this study, we excluded boar stations (i.e., facilities producing liquid boar semen for artificial insemination), cutting and processing plants since they were not involved in live animal movements and thus played a limited role in transmitting infectious diseases among live pigs. Holdings could be assigned multiple labels if they reported different activities or no label at all if they did not report any activity for the year (these were classified as “inactive” for the considered period).

The holdings’ geographical coordinates were overlaid over a shapefile of Austrian municipalities (Statistik Austria) using the R package *sf* (Pebesma, 2018). We extracted the name of the municipality where each holding was located using the function *st\_join()*. Due to the 5-kilometer radius randomization of coordinates, some holdings fell outside the boundaries of Upper Austria. To correct for this, we employed a k-Nearest Neighbor join method (function *st\_nn()*, with  $k = 1$ ), which assigns the attributes of the closest polygon to a point, available in the package *nngao* (Dorman, 2023).

## Network analysis

To create the weighted networks, we assigned two types of edge weights: (i) trade frequency: each edge represents one transaction with a weight of 1, regardless of the number of pigs involved; (ii) trade volume: each edge is assigned a weight equal to the number of pigs traded during that exchange (i.e., batch volume). The edge direction corresponded to a movement *from* the source holding to the destination holding. We created two static representations of each network by aggregating daily movement data throughout 2021. This process yielded multigraphs, where multiple edges could exist between pairs of nodes. These multigraphs were subsequently converted into simple graphs by collapsing multiple edges into single weighted edges. The resulting edge weights corresponded to either (i) the total number of trades (frequency-based network) or (ii) the total number of animals traded (volume-based network) between pairs of nodes. In both networks, a higher edge weight between two nodes corresponded to a shorter “distance” between them, signifying a stronger connection. These two representations of the Upper Austrian pig trade network are *isomorphic*, meaning they share identical underlying structures and node connections (Wasserman and Faust, 1994).

### Quantifying similarities and differences between networks

We normalized the edge weights in each network by dividing them by the maximum value of the edge weights within that specific network (Antonioni and Tsompa, 2008). This normalization ensured both networks were on a comparable scale, facilitating a fair comparison.

To characterize and compare the frequency- and volume-based networks, we computed the following weighted network-level centrality metrics, as suggested by Bellingeri et al. (Bellingeri et al., 2023): clustering coefficient (McCassey and Bijma, 2015), average path length (West et al., 2001), and diameter (West et al., 2001). The clustering coefficient quantifies the density of triangles in a network, representing the probability that two neighbors of the same node are themselves connected. Average path length is the mean number of steps along the shortest paths between all pairs of nodes. Diameter refers to the longest shortest path among all connected node pairs in the network (West et al., 2001; Wasserman and Faust, 1994; McCassey and Bijma, 2015).

We also computed three node centrality metrics: strength (Barrat et al., 2004), betweenness (Freeman, 1978), and closeness centrality (Marchiori and Latora, 2000). These metrics were selected based on their direct and functional relevance to animal trade flows and disease transmission. Specifically, strength, defined as the sum of edge weights connected to a node, captures the total volume or frequency of animals traded and reflects the node’s overall activity in the network. Betweenness centrality measures how often a node lies on the shortest paths between other nodes, indicating its potential to act as a bridge between otherwise disconnected parts of the network. Closeness centrality, which quantifies the average distance from a node to all others, reflects how quickly a holding can reach – or be reached by – others through direct or indirect trade connections (Wasserman and Faust, 1994; Freeman, 1978; Keeling and Rohani, 2011).

Closeness and betweenness centrality rely on the concept of shortest paths. However, in weighted networks of livestock movements, edge weights represent the strength of the connection between a pair of holdings rather than a cost or distance. Therefore, to ensure that higher trade frequencies or volumes translated into shorter distances (reflecting stronger connections), we inverted the edge weights when calculating weighted closeness and betweenness centrality, as proposed by Newman (Newman, 2001) and Brandes (Brandes, 2001).

We compared the distributions of edge weights and node centrality metrics (strength, closeness, and betweenness) in both the frequency-based and volume-based networks using density plots. To evaluate the similarity of edge weights between the two networks, we ranked edges

by weight within each network and applied a Kendall rank correlation test with a significance level set to 0.05 (Ghanem et al., 2019).

To assess the consistency of node importance across centrality metrics, we performed pairwise comparisons of holding (node) rankings based on the three centrality metrics within each network and across the two network types using the Kendall rank correlation test (Ghanem et al., 2019).

Additionally, we investigated whether specific types of pig holding activities were associated with higher node centrality. For each activity type, we computed the median centrality values and tested for group differences using the Kruskal–Wallis test. When holdings were associated with multiple activities, they were included in the analysis under each applicable label.

### Community detection

A community is defined as a group of nodes with denser connections (trades) among themselves than with the rest of the network (Radicchi et al., 2004). We used the Leiden algorithm, which iteratively (i) optimizing modularity, (ii) refine the partition, and (iii) aggregates communities. We selected this algorithm because it improves upon Louvain method by guaranteeing well-connected communities, therefore ensuring better partition quality, and more reliable communities. Additionally, the Leiden algorithm converges faster and scales better to very large graphs (Traag et al., 2019).

Community detection was performed at two levels: (i) holding-level: we applied the Leiden algorithm to the previously described network of pig trades, where nodes represented individual holdings and edges captured direct trade relationships between them; (ii) municipality-level: we first aggregated holdings based on their municipality (nodes = municipalities, edges = inter-municipality movements). In both networks, edge weights were assigned to represent either the frequency of trades or the volume of pigs traded.

We quantified the similarities in community membership using the matching method (Hopcroft et al., 2004), where matching values range from 0 (no overlap) to 1 (identical membership). We compared the community structures between frequency- and volume-based networks by evaluating holding/municipality composition, size, and spatial connectivity patterns.

### Epidemics on weighted networks

#### Spreading dynamic

We aimed to identify influential nodes by ranking them based on their epidemic “susceptibility”, defined as the likelihood of infection during a contagion process. Specifically, we focused on identifying nodes infected more frequently than average and assessed whether node ranking, based on “susceptibility”, differs between frequency-based and volume-based networks and whether these results align with centrality-based rankings.

We simulated epidemic spread on both networks using a stochastic Susceptible–Infectious–Recovered–Susceptible (SIRS) model. While temporal analyses more accurately reflect real-world transmission processes, they introduce substantial variability in node rankings across different time windows. Here, we chose a static approach to prioritize interpretability for surveillance applications.

In our model: transitions between states were determined probabilistically at each time step; pig movements, represented by edges, indicate direct contact between pig operations, through which herds can be infected; each holding occupied states  $S$ ,  $I$ , or  $R$ ; infection may occur when an infectious holding sends pigs to a susceptible one; infected holdings temporarily cease trading before restocking and returning to state  $S$ .

The model incorporated the recovery rate (transition from  $I$  to  $R$ ), denoted  $\gamma$ , and the transition rate from  $R$  to  $S$ , denoted  $\sigma$ . The infection probability (transition from  $S$  to  $I$ )  $\lambda_i$  for susceptible node  $i$  depends on

weighted connections to infectious nodes, with edge types denoted as  $\xi \in \{\text{trade frequency, batch size}\}$ . The infection probability (transition from S to I)  $\lambda_i$  for susceptible holding  $i$  at each time step is:

$$\lambda_i = 1 - \exp\left(-\beta \sum_{j=1}^{n_i} I_j w_{\xi_{i,j}}\right) \quad (1)$$

where:

- $\beta$ : transmission rate that depends on the edge weight  $w_{\xi}$  (frequency or volume of trades)
- $I_j$ : binary indicator ( $I_j = 1$  if neighbor  $j$  is infectious, 0 otherwise)
- $w_{\xi_{i,j}}$ : edge weight (frequency or volume of trades) between node  $i$  and neighbor  $j$
- $n_i$ : neighbors of node  $i$

In our main analysis, we set the following values:  $\beta = 0.5$ ,  $\gamma$  ranged from 5 to 10 days (allowing sufficient spread), and  $\sigma$  ranged from 10 to 30 days (based on the scientific opinion of the European Food Safety Authority (EFSA) Panel on Animal Health and Welfare (Nielsen et al., 2021)). We selected the  $\beta$  value based on Büttner et al. (Büttner and Krieter, 2021), where high transmission probability led to a convergence in the number of infected farms across differently weighted networks.

We initialized outbreaks by randomly selecting one infected holding per previously identified community (holding-level), excluding abattoirs, running 1,000 simulations per community (where the epidemic could start) for 90 days. This approach (see S1 Text) (i) ensured that the seeding of the infection occurs with equal probability across all communities, (ii) captured the critical exponential growth phase of the outbreak (a critical window for intervention) while (iii) maintaining computational efficiency.

We evaluated the overall impact of the epidemic by calculating the average number of infected holdings across all simulations (epidemic size) and the average number of communities reached by the epidemic (S2 Text).

#### Node ranking based on nodes' susceptibility

To quantify node susceptibility, we counted the number of times each node  $i$  in community  $C_j$  was infected/reinfected across 1,000 simulations, storing these values in a vector  $V_{i,j} = (n_{i,j,1}, \dots, n_{i,j,1000})$ , where  $n_{i,j,k}$  represents the number of (re)infections for node  $i$  in simulation  $k$  ( $i = 1, \dots, N$ ;  $j = 1, \dots, M$ ;  $k = 1, \dots, 1000$ ).

Next, we computed the average infection frequency for node  $i$

$$I_i = \frac{1}{1000} \sum_{k=1}^{1000} n_{i,j,k}, \quad (2)$$

$I_i$  was used to rank the nodes based on their epidemic susceptibility (simulation-based ranking). This ranking served as the benchmark for comparison with centrality-based rankings.

We assessed agreement between simulation- and centrality-based rankings using Kendall rank correlation tests. Nodes in the top 5% of the best-correlated centrality metric were considered potential sentinel surveillance holdings. We analyzed their spatial distribution using point pattern analysis (Weil, 2007) to detect clustering patterns (see S3 Text for methodological details).

#### 2.0.1. Sensitivity analysis

We conducted a sensitivity analysis to assess the robustness of node ranking correlations under varying transmission scenarios. Four transmission rates  $\beta$  were tested: 0.1, 0.3, 0.7, and 0.9, spanning low to high transmissibility. For each scenario, we calculated the Kendall rank correlation coefficient in both frequency- and volume-based networks, evaluating metrics consistency across transmission intensities.

Additionally, epidemic impact was quantified through multiple complementary metrics: (i) average node susceptibility: mean infection frequency [95% CI], (ii) ranking consistency: Kendall's  $\tau_b$  between network types; (iii) community effects: Kruskal–Wallis test for seeding location impact; (iv) epidemic facilitation: Dunn's test, (v) outbreak magnitude; Wilcoxon test for median epidemic size; and (vi) community with highest vulnerability.

#### Software

Data cleaning, preparation, subsequent data analyses, and computation of the figures were performed in R software (v.4.1.0) (R Core Team, 2021) using RStudio Server “Juliet Rose” (v.1.4.1717) (RStudio Team, 2020). The network analysis and study of the spreading dynamics was performed using the R package igraph (Csárdi et al., 2024). Community detection using the Leiden algorithm was conducted using `leidenAlg` (Kharchenko et al., 2022). Point pattern analysis was performed with `spatstat` (Baddeley and Turner, 2005).

### 3. Results

#### The pig trade network in Upper Austria

In 2021, there were 110,891 movements recorded in Upper Austria involving 6,020 pig holdings, with most holdings geographically concentrated in the central region (Fig. 1). For this study, we focused on the 92,914 (83.8%) movements that occurred exclusively within the federal state of Upper Austria, representing trades among 5,766 holdings (95.8% of all regional operations). The remaining 254 holdings (4.2%) conducted trades crossing federal state or national boundaries and were excluded from analysis. The intra-state network included 5,726 (99.3%) farms, 288 (5%) abattoirs, 96 (1.6%) trading points, and 14 (< 1%) collection points. Overall, these transactions involved 3,100,852 pigs, with nearly equal proportions destined for slaughter (1,510,690; 49%) versus transfers between animal operations (1,590,162; 51%).

#### Comparison of the edge weight distributions

The frequency-based network exhibited trade frequencies between pairs of pig operations (edge weights) ranging from 1 to 99, with a median of 2. The volume-based network showed edge weights (total pigs exchanged) spanning 1 to 9,384 animals (median = 26), with 896 edges (5.5%) accounting for half of all traded animals. These figures reveal that while most holdings engaged in infrequent, low-volume exchanges during the studied period, a small subset exhibited high-frequency, high-volume trading relationships.

The edge weight distribution differed between the frequency- and volume-based networks. Specifically, the frequency-based network showed a clear bimodal edge weight distribution, whereas the volume-based network exhibited a more uniform pattern (Fig. 2). Despite these distributional differences, the Kendall test showed a strong positive correlation in edge-weight rankings between networks (Kendall  $\tau_b$  correlation coefficient = 0.56;  $p < 0.001$ ), indicating consistent ordering of edge weights across both networks.

#### Network centrality statistics

The frequency- and volume-based networks exhibited similar clustering coefficients:  $8.9 \times 10^{-3}$  versus  $8.7 \times 10^{-3}$ , respectively. However, their connectivity patterns differed substantially: the frequency-based network showed longer path characteristics (average path length = 1.6, diameter = 6.97) whereas the volume-based network demonstrated more direct connectivity (average path length = 0.3, diameter = 4.09) (Table 1).

These findings indicate that holdings were typically connected by fewer than two links in the frequency-based network or one link in the volume-based network, on average. In the frequency-based network, the most distant pair of holdings requires seven intermediaries to connect; in contrast, the volume-based network reveals far more direct routes.

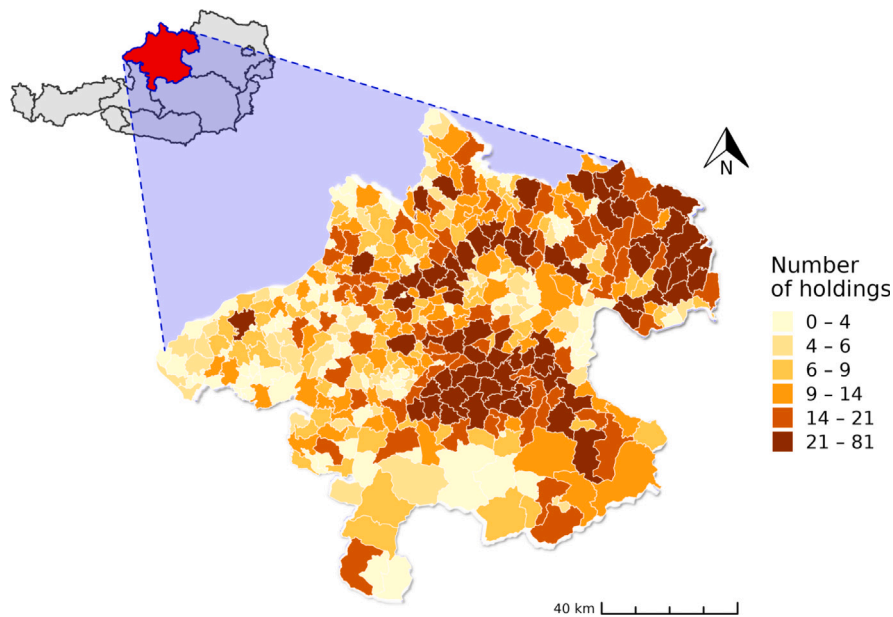


Fig. 1. Density of pig holdings per municipality in the federal state of Upper Austria, Austria, 2021.

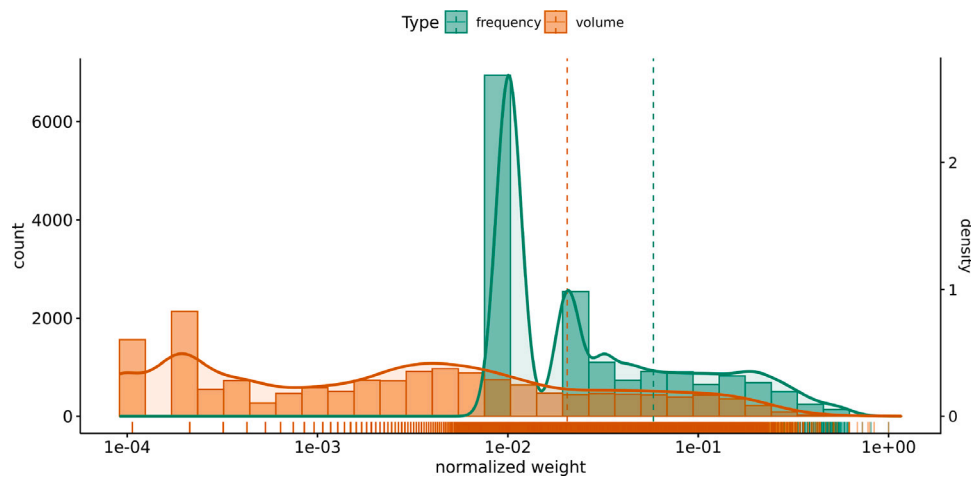


Fig. 2. Edge weight distribution in the frequency- (green) and volume-based network (red) of pig trade in Upper Austria, 2021, normalized, in each network, by the maximum edge value. The dashed lines and marginal rugs represent the means and marginal distribution for each network, respectively. The x-axis is presented in a log scale. (For interpretation of the references to color in this figure legend, the reader is referred to the web version of this article.)

**Table 1**  
Network-level measures calculated for the frequency- and volume-based representations of the Upper Austrian pig trade network, Austria, 2021.

Metric	Frequency-based	Volume-based
Clustering coefficient	$8.9 \times 10^{-3}$	$8.7 \times 10^{-3}$
Average path length	1.6	0.3
Diameter	6.97	4.09

Clustering coefficient, average path length, and diameter for both the frequency- and volume-based pig trade networks in Upper Austria, Austria, 2021.

### Community detection

#### Holding-level community detection

The Leiden algorithm identified 46 and 80 trade communities within the frequency- and volume-based networks, respectively. These communities were characterized by high spatial fragmentation, often comprising fewer than five holdings each (see S1 Text). This output was not further considered in this study, as the focus was on larger, more interconnected communities that could offer meaningful insights into pig

trade dynamics and network structures, particularly for epidemiological purposes.

#### Municipality-aggregated network

The Leiden algorithm identified six trade communities in both the frequency- and volume-based municipality networks (Fig. 3). The low matching coefficient,  $0.22 \pm 0.29$  (standard deviation, SD), revealed substantial differences in community memberships between network representations. Distinct spatial patterns emerged: the frequency-based network displayed clear geographic segregation with well-defined community boundaries (Fig. 3A). Conversely, the volume-based network exhibited fragmented communities without distinct “blocks” (Fig. 3B). While eastern and southern regions maintained consistent community membership across both networks, northern, central, and western regions exhibited varying community memberships. Spatially isolated municipalities (those geographically separated from their assigned communities) typically connected by single trade to their community (Fig. 3).

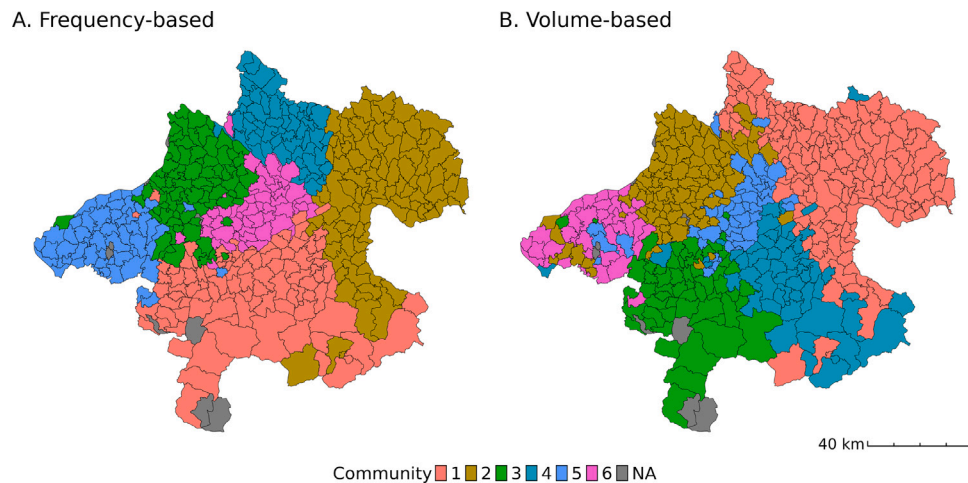


Fig. 3. Pig trade communities in Upper Austria, Austria, 2021, detected using the Leiden algorithm run on the municipality network. (A) Frequency-based network. (B) Volume-based network. The municipality is considered as the epidemiological unit.

### Ranking of nodes based on centrality metrics

Kendall's analysis revealed strong correlations between node rankings based on strength and closeness centrality in both networks ( $\tau_b = 0.75$  for frequency-based;  $\tau = 0.84$  for volume-based;  $p < 0.001$ ). Correlations between closeness and betweenness rankings were lower but significant ( $\tau_b = 0.35$ ;  $p < 0.001$  for both networks). Strength and betweenness ranking displayed moderate correlations ( $\tau_b = 0.47$  for frequency-based;  $\tau = 0.42$  volume-based;  $p < 0.001$ ). These findings showed that betweenness correlates weakly with the two other measures (Fig. 4).

Comparison between networks showed strong correlation between strength rankings ( $\tau_b = 0.8$ ,  $p < 0.001$ ), with 107 nodes shared between the top 5% (counting 289 nodes) of both networks. Density plots revealed bimodal distributions of the node strength (Fig. 5A), with a notable proportion of nodes showing lower strength centrality in the volume-based network, while most of the nodes in the frequency-based had average values.

The closeness centrality rankings also showed strong agreement between network types ( $\tau_b = 0.75$ ,  $p < 0.001$ ), with 148 (51%) common nodes appearing in the top 5% of both networks, and closeness centrality distributions exhibited bimodal patterns with some overlap (Fig. 5B).

Betweenness centrality showed the strongest inter-network correlation ( $\tau_b = 0.86$ ,  $p < 0.001$ ), with 244 (85%) shared top nodes. The density plots showed bimodal distribution, but left-skewed, with a notable overlap, confirming highly similar distributions of node betweenness across networks (Fig. 5C).

The Kruskal–Wallis test confirmed significant differences in centrality metrics between operation types ( $p < 0.001$ ). In both networks, collection points consistently showed high median centrality across all three metrics. On the other hand, slaughterhouses had high median strength and closeness but lower betweenness centrality (Table 2), reflecting their role as endpoints in the trade chain. Farms generally exhibited lower median centrality values, corresponding to their low trade frequencies and volumes compared to specialized operations like collection points (frequently receiving and sending large volumes of pigs) and abattoirs (frequently receiving large volumes of pigs for slaughter).

### Rankings of nodes based on epidemic susceptibility and epidemic size

Our simulations revealed that epidemics consistently spread beyond their origin communities in both network types, with no observed cases

of complete intra-community containment. This pattern of between-community transmission persisted across all outbreak scenarios (S2 Text).

In the frequency-based network, nodes were infected on average 0.022 times per simulation (95%CI: 0.020–0.023); compared to 0.017 (95%CI: 0.016–0.018) in the volume-based network. The strong positive correlation between simulation-based rankings across networks ( $\tau_b = 0.678$ ,  $p < 0.001$ ) indicates a consistent identification of influential nodes regardless of weighting scheme.

The epidemic size (i.e., average number of infected nodes across 1,000 simulations) varied significantly by seeding community in both networks (Kruskal–Wallis test:  $\chi^2 = 779.41$ ,  $df = 5$ ,  $p < 2.2 \times 10^{-16}$ ). Post-hoc analysis using Dunn's test revealed consistent patterns across network types. Community 5 showed the least facilitation (smallest outbreaks when seeded) and least vulnerability (it consistently showed the fewest secondary infections when any other community is seeded). Community 6 proved to be the most facilitative, generating the largest epidemics across all communities when seeded. Communities 1 and 3 were consistently the most vulnerable receivers, exhibiting the highest attack rates irrespective of where the epidemic began. Wilcoxon signed-rank tests revealed that volume-based networks had significantly larger median epidemic sizes than frequency-based networks ( $p < 0.005$ ).

### Centrality- versus simulation-based rankings

Both frequency- and volume-based networks showed weak positive correlations between simulation-based rankings and all three centrality measures (Table 3). In both network representations, strength centrality-ranking exhibited the highest correlation with the simulation-based ranking.

Analysis of the top 5% of nodes (289 nodes) revealed a stronger positive correlation between strength centrality- and simulation-based rankings compared to the full node set. In contrast, closeness centrality showed lower agreement for these highest-ranked nodes. Since the strength-based ranking consistently showed the strongest correlation, we focused our subsequent analysis on the top 5% highest-ranked nodes identified by strength centrality for sentinel surveillance evaluation.

In the frequency-based network, these top-ranked nodes were distributed across communities as follows: community 1 (113 nodes), community 2 (50), community 3 (45), community 4 (16), community 5 (8), and community 6 (57). The volume-based network showed a similar but distinct distribution: community 1 (107 nodes), community 2 (14), community 3 (84), community 4 (31), community 5 (15), and community 6 (38), with 107 nodes common to both networks' top rankings.

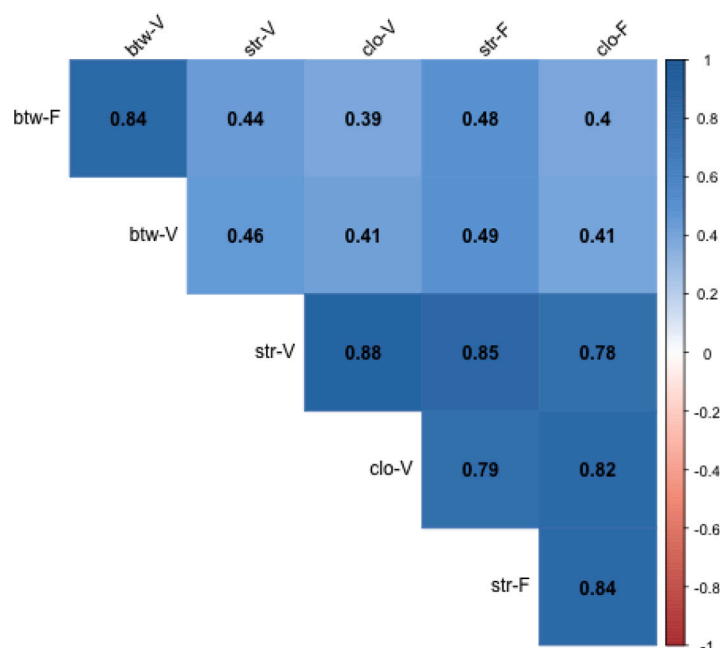


Fig. 4. Upper matrix of pairwise Kendall's tau rank correlations between node rankings based on three weighted centrality metrics (strength; str; closeness: clo; betweenness: btw) within and between the frequency-based (denoted F-) and volume-based (V-) representations of the Upper Austrian pig trade network, 2021. The Kendall-tau correlation coefficient can take values from  $-1$  to  $1$ , where the most positive value reflects a positive correlation between ranks.

Table 2

Node centrality values for both the frequency- and volume-based networks of pig movements in Upper Austria, Austria, 2021.

Type of holdings	Frequency-based ( $\times 10^{-2}$ )			Volume-based ( $\times 10^{-2}$ )		
	Strength	Closeness	Betweenness	Strength	Closeness	Betweenness
Trade point	3.3	47.1	3.1	2.2	29	3.9
Slaughterhouse	2.2	38.2	0.37	1.5	17	0.42
Farms	0.3	36.1	0.08	0.24	19.5	0.1
Collection point	5.7	54.7	9.4	5.9	46	13.1

Median values of the node strength, closeness, and betweenness centrality for different types of node: trade points, slaughterhouses, and farms, in the frequency- and volume-based pig trade networks in Upper Austria, 2021.

Point pattern analysis demonstrated spatial clustering of these potential sentinels compared to Complete Spatial Randomness in both networks (Figure 3 in S3 Text) ( $p$  - values  $< 0.005$ ). Notably, sentinels identified in the volume-based network showed tighter clustering patterns than those from the frequency-based network (S3 Text).

### 3.0.1. Sensitivity analysis

The epidemic impact metrics for all transmission scenarios are detailed in S1 Table. Two key patterns emerged from our sensitivity analysis:

(i) Strength centrality robustness: Across all transmission scenarios, strength ranking maintained a consistently positive yet modest correlation with simulation-based rankings ( $\tau = 0.14$ – $0.31$ , all  $p < 0.001$ ). While correlation strength exhibited a slight negative association with increasing transmissibility, statistical significance persisted across all scenarios. (ii) Top-node performance: For the top 5% highest-ranked nodes, strength ranking maintained strong agreement with simulation-based rankings (Kendall's  $\tau_b$ :  $0.42$ – $0.61$ , all  $p < 0.001$ ).

## 4. Discussion

Before epidemiological inferences (e.g., transmission dynamics, risk prioritization) can be reliably applied to livestock networks, methodological ambiguities in network construction, particularly edge-weighting choices, must be resolved. Our study advances network epidemiology by systematically isolating the effects of edge-weighting choices on node importance in disease spread. Using isomorphic pig

trade networks weighted by either trade frequency or volume, we demonstrate that strength centrality robustly identifies high-risk holdings across both weighting schemes, outperforming betweenness and closeness centrality when validated against 6,000 stochastic SIRS simulations. This finding is particularly valuable when movement data is incomplete, as they demonstrate that frequency-based networks-even without volume data-can reliably identify high-risk holdings for targeted disease surveillance. Moreover, while prior work established that weighting affects epidemic size in livestock movement network (Büttner and Krieter, 2021; Candeloro et al., 2016; Schley et al., 2012), we reveal three additional dimensions: weighting scheme alters network path metrics, community structure (46% municipality membership shifts), and edge weight distributions (bimodal vs. uniform), with critical implications for targeted surveillance.

The higher path metrics (average path length and diameter) in the frequency-based network indicate that transmission chains driven solely by trade counts will unfold over longer, more circuitous paths, potentially slowing pathogen spread but demanding broader surveillance. Conversely, the volume-based network behaves as a densely connected structure, enabling pathogens to traverse the system in fewer steps and achieve rapid, wide-scale dissemination (Dubé et al., 2009; Wasserman and Faust, 1994; Pérez-Ortiz et al., 2022). This structural difference is reflected in our simulation results, which showed that the volume-based network consistently produced larger outbreaks compared to the frequency-based one. Consequently, control strategies informed solely by trade frequency risk underestimating the velocity, spatial extent, and size of epidemics driven by large-batch shipments,

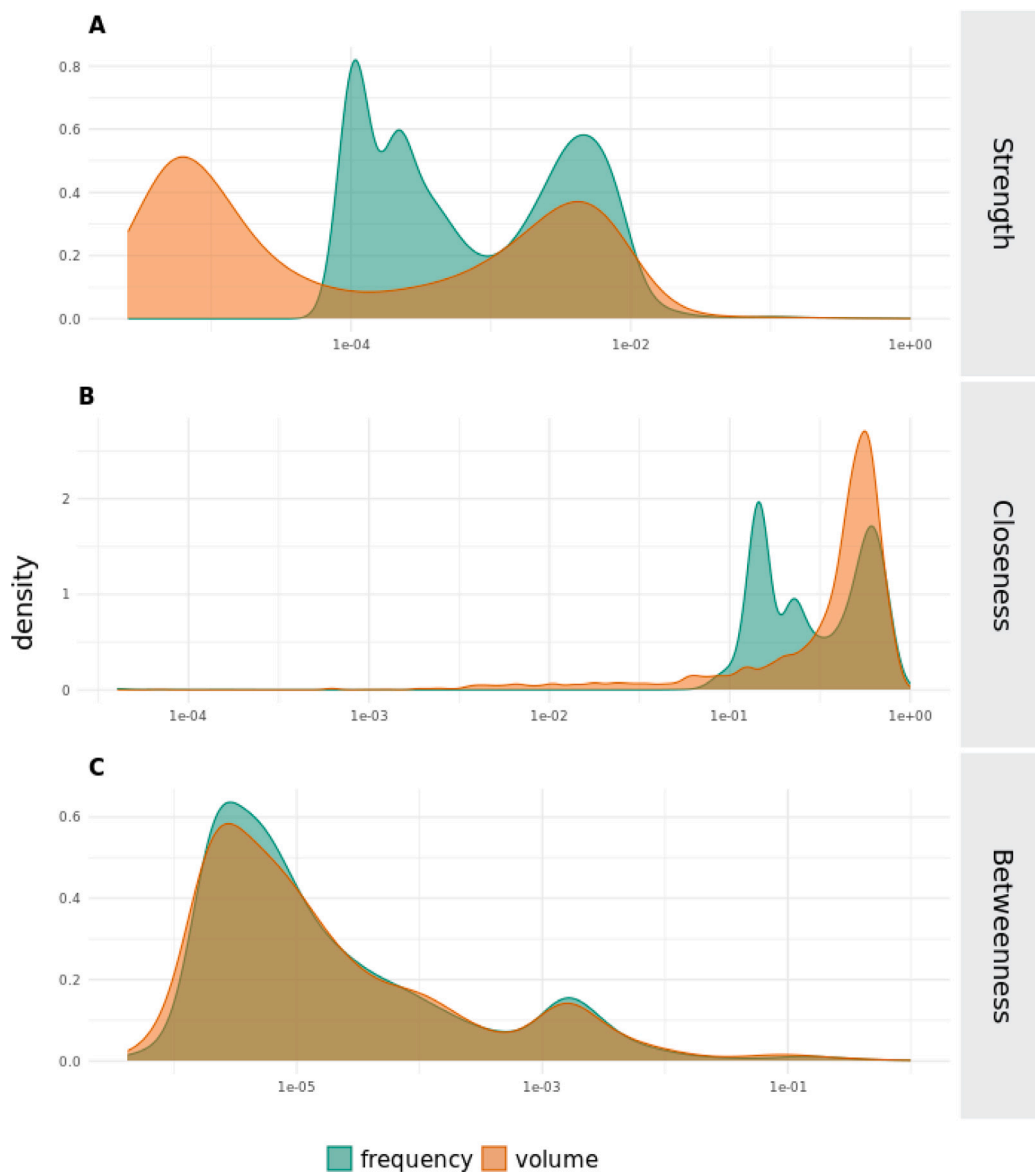


Fig. 5. Density plots showing the distributions of the weighted node centrality metrics (A) strength, (B) closeness, and (C) betweenness for both the frequency- and volume-based networks of pig movements in Upper Austria, Austria, 2021.

underscoring the necessity of incorporating volume-based metrics into surveillance and intervention planning (Lysholm et al., 2025; Büttner et al., 2013; Lentz et al., 2016). While the frequency-based network exhibited a clear bimodal edge-weight distribution, the volume-based network had a more uniform distribution. Nevertheless, edge rankings were highly correlated across networks, indicating that pairs of holdings that traded frequently also tend to trade larger volumes. Therefore, prioritizing the highest-ranked edges, regardless of whether they are defined by trade count or batch size, is crucial for identifying the most influential transmission pathways in disease control (Rautureau et al., 2011; Büttner et al., 2013; Büttner and Krieter, 2018).

We also found strong positive correlation in node centrality rankings (strength, closeness, and betweenness) within and between the two networks, indicating that (i) multiple centrality measures may redundantly capture similar aspects of node importance (Valente et al., 2008) and (ii) both networks shared similar topological properties. However, betweenness centrality consistently exhibited weaker correlations with closeness and strength centrality. This discrepancy may arise because betweenness identifies nodes that serve as bridges connecting different parts of the network, whereas closeness and strength emphasize nodes

with central locations and strong connections, respectively (Wasserman and Faust, 1994; Newman, 2018).

Collection points consistently showed high centrality values across all three metrics in both networks, indicating their central role in the networks (Robinson and Christley, 2007; Natale et al., 2009; Rautureau et al., 2011), irrespective of edge weighting. These nodes function as bridge, facilitating numerous transactions (Newman, 2018). On the other hand, farms and slaughterhouses exhibited low betweenness centrality, consistent with the typical unidirectional flow of the pig trade network and the terminal role of slaughterhouses in the pork production.

Epidemic simulations (SIRS model) used to rank epidemic susceptibility revealed a strong correlation between the two networks, suggesting that edge weight has minimal impact on identifying vulnerable nodes. In other words, nodes most susceptible to infection remained largely consistent, regardless of whether frequency or volume was used to weight interactions.

Among centrality measures, strength centrality, which integrates both the number of connections and their weights (Wasserman and Faust, 1994; Newman, 2018), exhibited the strongest and more robust

**Table 3**

Comparison of node rankings based on three centrality metrics versus simulation-based rankings, for both the frequency- and volume-based networks of pig movements in Upper Austria, Austria, 2021.

Transmission rate $\beta$	Network	Centrality	Full network		Top 5% highest-ranked	
			$\tau$	p-value	$\tau$	p-value
0.1	Frequency-based	Betweenness	0.29	< 0.001	0.05	0.5022
		Closeness	0.27	< 0.001	0.36	$4.018 \times 10^{-6}$
		Strength	0.31	< 0.001	0.61	$2.084 \times 10^{-11}$
	Volume-based	Betweenness	0.28	< 0.001	0.15	0.0471
		Closeness	0.26	< 0.001	0.17	0.02514
		Strength	0.29	< 0.001	0.42	$3.539 \times 10^{-07}$
0.3	Frequency-based	Betweenness	0.21	< 0.001	0.14	0.07144
		Closeness	0.17	< 0.001	0.28	0.0005378
		Strength	0.22	< 0.001	0.58	$1.543 \times 10^{-11}$
	Volume-based	Betweenness	0.25	< 0.001	0.17	0.03427
		Closeness	0.24	< 0.001	0.05	0.541
		Strength	0.26	< 0.001	0.46	$1.489 \times 10^{-8}$
0.5	Frequency-based	Betweenness	0.15	< 0.001	0.08	0.338
		Closeness	0.13	< 0.001	0.08	0.343
		Strength	0.16	< 0.001	0.51	< 0.001
	Volume-based	Betweenness	0.15	< 0.001	0.2	0.02396
		Closeness	0.17	< 0.001	-0.02	0.7753
		Strength	0.17	< 0.001	0.5	< 0.001
0.7	Frequency-based	Betweenness	0.19	< 0.001	0.09	0.2923
		Closeness	0.16	< 0.001	0.17	0.05267
		Strength	0.20	< 0.001	0.47	$3.504 \times 10^{-8}$
	Volume-based	Betweenness	0.28	< 0.001	0.11	0.1467
		Closeness	0.27	< 0.001	0.11	0.1355
		Strength	0.29	< 0.001	0.38	$4.121 \times 10^{-6}$
0.9	Frequency-based	Betweenness	0.18	< 0.001	0.17	0.06508
		Closeness	0.16	< 0.001	0.28	0.005459
		Strength	0.19	< 0.001	0.49	$2.465 \times 10^{-8}$
	Volume-based	Betweenness	0.24	< 0.001	0.16	0.06612
		Closeness	0.23	< 0.001	-0.04	0.6363
		Strength	0.25	< 0.001	0.47	$9.716 \times 10^{-8}$

Kendall's tau and associated p-values comparing node rankings based on betweenness, closeness, and strength centrality with epidemic-derived susceptibility rankings in frequency- and volume-based networks.

correlation with simulation-derived susceptibility rankings. This consistency persisted across both weighting schemes and all tested transmission rates. The correlation strength notably increased when analyzing the top 5% highest-ranked nodes, making strength centrality a valuable tool for identifying vulnerable holdings in the network, i.e., those frequently involved in disease transmission. These findings align with earlier studies in pigs (Passafaro et al., 2020; Wiratsudakul et al., 2022), cattle (Candeloro et al., 2016), and sheep networks (Schley et al., 2012), confirming that strength centrality robustly captures node influence across different weighting schemes, making it particularly valuable for targeted surveillance program design.

The weaker correlation observed across the full set of nodes is due to the instability of the rankings' tails, influenced by a large number of holdings that infrequently engaged in trades or involved relatively small volumes of animals. Similar observations of pig operations with sporadic trading patterns have been documented in pig (Büttner and Krieter, 2021; Lentz et al., 2016; O'Hara et al., 2022; Passafaro et al., 2020), cattle (Volkova et al., 2010a; Rautureau et al., 2011), and sheep trade networks (Volkova et al., 2010b).

Our research identified a structural divergence in network behavior depending on the data aggregation level. At the holding level, both frequency- and volume-based networks exhibited low modularity, reflecting diffuse and broadly distributed connectivity patterns. In contrast, when aggregated at the municipality level, the same networks showed high modularity, indicating strong community segregation and more compartmentalized trade structures. Spatial analysis of the top 5% influential holdings (by strength centrality) showed significant clustering across Upper Austria, yet uneven distribution across communities within the municipality-networks. This dual pattern (local clustering within broader regional dispersion) supports their utility as sentinels,

as local clustering ensures monitoring efficiency and cross-community distribution provides outbreak detection coverage. These findings align with the work of Colman et al. (Colman et al., 2019), who suggested that in highly modular networks, such as those observed at the municipality level, sentinel surveillance is most effective when sampling efforts are distributed across different regions or communities.

Epidemic size varied significantly depending on which community was initially seeded, in both networks. On average epidemic size was significantly higher in the volume-based network. This pattern may be driven by "weak ties" (infrequent or low-volume trades connecting distant parts of the network) that act as bridges facilitating spread across communities. These results exemplify the 'strength of weak ties' paradox (Granovetter, 1973; Burt, 2004), where infrequent or low-volume exchanges serve as crucial connectors that link otherwise distant communities.

This study presents some limitations. First, it focuses on the pig trade network in Upper Austria, thus findings may not generalize to other regions. Additionally, we limited our analysis to three centrality metrics and did not include alternative centrality measures such as eigenvector centrality or PageRank, as these prioritize "prestige" (i.e., being connected to other well-connected nodes) over actual trade volume or frequency (Newman, 2018). While useful in certain types of networks, these metrics are less appropriate in the context of direct physical movements of livestock, where functional roles in transmission dynamics are more relevant than influence by association (Bucur and Holme, 2020; Natale et al., 2009). Therefore, strength, betweenness, and closeness were most aligned with our aim to identify holdings critical for surveillance and control. Nonetheless, we acknowledge that alternative or hybrid centrality approaches may offer valuable insights in future work.

Second, we assumed that all pig movements were accurately recorded, as movement reporting is mandatory under the Animal Health Law (AHL, Regulation (EU) 2016/429) (European Parliament and The Council, 2016). While some underreporting cannot be entirely ruled out, we expect it to be minimal and unlikely to substantially affect the network structure or the overall findings of this study. Additionally, incorporating additional holding attributes, such as biosecurity or herd size, could improve the model and susceptibility rankings.

A further limitation stems from our use of a static network approach, which aggregates temporal trade data into a single snapshot. This approach overlooks dynamic aspects of pig movements that vary seasonally or temporally (Lentz et al., 2016). This static representation could lead to two key limitations: (i) the aggregation process may artificially inflate predicted epidemic size (Enright and Kao, 2018; Holme, 2005; Lentz et al., 2016), by assuming all recorded connections are simultaneously active; and (ii) from an epidemiological standpoint, our approach implies that all contacts are persistent, while in reality many transmission opportunities are transient (Kim and Anderson, 2012). This simplification may affect the accuracy of both centrality measures and simulated spread patterns. Future studies comparing static and dynamic network approaches could provide additional insights into how trade timing interacts with weighting choices to influence disease spread.

Lastly, while strength centrality is promising, its practical implementation must be considered. If rankings based on centrality metrics change over time, stakeholders may face challenges in adapting surveillance efforts to these evolving rankings. However, increasing model complexity may reduce usability for surveillance personnel. Therefore, while dynamic networks are very valuable (Oetershagen et al., 2022), their real-world usability should be balanced against interpretability and ease of use to ensure they remain manageable for those performing surveillance.

## 5. Conclusion

Our findings have practical implications for developing more effective surveillance strategies. The strong alignment of strength centrality rankings with simulation-based ranking suggests that this metric can be a reliable and computationally efficient initial approach for identifying influential nodes in a static network. However, further validation using dynamic network models is recommended to confirm its reliability under dynamic conditions.

A network-based approach can enhance the efficiency of traditional surveillance strategies, by enabling more targeted, risk-based monitoring that is both actionable and field-deployable. While both frequency- and volume-based networks exhibited similar overall structures, our results clearly demonstrate that the choice of edge weighting significantly influences epidemic size. This underscores the importance of tailoring edge weight selection to the characteristics of the infectious disease under surveillance (or being modeled), notably its transmission probability and mode of spread.

In conclusion, the weighted network approach holds considerable potential for informing targeted surveillance and control strategies. By prioritizing high-risk nodes through strength centrality and accounting for the differences between frequency- and volume-based weighting, animal health authorities can implement more efficient and cost-effective interventions.

## CRediT authorship contribution statement

**Gavrila A. Puspitarani:** Writing – review & editing, Methodology, Visualization, Investigation, Conceptualization, Writing – original draft, Formal analysis. **Yan-Shin Jackson Liao:** Writing – original draft, Investigation, Visualization, Conceptualization, Methodology, Formal analysis. **Reinhard Fuchs:** Writing – review & editing, Data curation. **Amélie Desvars-Larrive:** Writing – original draft, Methodology, Supervision, Writing – review & editing, Conceptualization.

## Funding sources

This research did not receive any specific grant from funding agencies in the public, commercial, or not-for-profit sectors.

## Declaration of competing interest

The authors declare that they have no known competing financial interests or personal relationships that could have appeared to influence the work reported in this paper.

## Acknowledgments

The authors would like to thank the Austrian Federal Ministry of Social Affairs, Health, Care and Consumer Protection (BMSGPK) and the Austrian Agency for Health and Food Safety (AGES) for providing the data for this study. We also extend our gratitude to Andrea Ladinig and Klemens Fuchs, members of our advisory board, for their expert feedback and professional guidance. We also want to thank the Infectious Disease and One Health Erasmus Mundus Joint Master Degree for facilitating the internship of Yan-Shin Jackson Liao in our Group. Finally, we are grateful to our colleagues at the Complexity Science Hub for their valuable brainstorming sessions and continuous support.

## Appendix A. Supplementary data

Supplementary material related to this article can be found online at <https://doi.org/10.1016/j.epidem.2025.100849>.

**S1 Text. Holding-level community detection.** Results from the Leiden algorithm applied to the network of pig trades in Upper Austria, 2021, detailing the number of communities detected and the member count within each community.

**S2 Text. Disease spread within and across communities.** Analysis of epidemic spread dynamics to determine whether outbreaks remain within the initial community or extend to other communities.

**S3 Text. Point pattern analysis.** Analysis of the spatial distribution of the top 5% highest-ranked nodes based on strength centrality.

**S1 Table. Sensitivity analysis table.** Summary of key simulation and statistical-test results across transmission rates for frequency- and volume-based networks.

## Data availability

The metadata and R code used to produce the results are publicly available on Figshare at <https://doi.org/10.6084/m9.figshare.26494786.v1>. The raw data that support the findings of this study are available from the Austrian Federal Ministry of Social Affairs, Health, Care and Consumer Protection (BMSGPK) but restrictions apply to the availability of these data, which were used under license for the current study, and so are not publicly available. Data are however available from the authors upon reasonable request and with permission of the data owner.

## References

- Albert, R., Jeong, H., Barabási, A.-L., 1999. Diameter of the world-wide web. *Nature* 401 (6749), 130–131. <http://dx.doi.org/10.1038/43601>.
- Antoniou, I.E., Tsompa, E.T., 2008. Statistical analysis of weighted networks. *Discrete Dyn. Nat. Soc.* 2008, 1–16. <http://dx.doi.org/10.1155/2008/375452>.
- Baddeley, A., Turner, R., 2005. spatstat: An R package for analyzing spatial point patterns. *J. Stat. Softw.* 12 (6), 1–42. <http://dx.doi.org/10.18637/jss.v012.i06>.
- Barrat, A., Barthélemy, M., Pastor-Satorras, R., Vespignani, A., 2004. The architecture of complex weighted networks. *Proc. Natl. Acad. Sci.* 101, 3747–3752. <http://dx.doi.org/10.1073/pnas.0400087101>.
- Begon, M., Bennett, M., Bowers, R.G., French, N.P., Hazel, S.M., Turner, J., 2002. A clarification of transmission terms in host-microparasite models: numbers, densities and areas. *Epidemiol. Infect.* 129, 147–153. <http://dx.doi.org/10.1017/S0950268802007148>.

- Bellingieri, M., Bevacqua, D., Sartori, F., Turchetto, M., Scotognella, F., Alfieri, R., Nguyen, N.K.K., Le, T.T., Nguyen, Q., Cassi, D., 2023. Considering weights in real social networks: A review. *Front. Phys.* 11, <http://dx.doi.org/10.3389/fphy.2023.1152243>.
- Brandes, U., 2001. A faster algorithm for betweenness centrality. *J. Math. Sociol.* 25 (2), 163–177. <http://dx.doi.org/10.1080/0022250X.2001.9990249>.
- Bucur, D., Holme, P., 2020. Beyond ranking nodes: Predicting epidemic outbreak sizes by network centralities. *PLoS Comput. Biol.* 16, e1008052. <http://dx.doi.org/10.1371/journal.pcbi.1008052>.
- Burt, R.S., 2004. Structural holes and good ideas. *Am. J. Sociol.* 110, 349–399. <http://dx.doi.org/10.1086/421787>.
- Büttner, K., Krieter, J., 2018. Comparison of weighted and unweighted network analysis in the case of a pig trade network in Northern Germany. *Prev. Vet. Med.* 156, 49–57. <http://dx.doi.org/10.1016/j.prevetmed.2018.05.008>.
- Büttner, K., Krieter, J., 2021. Epidemic spreading in a weighted pig trade network. *Prev. Vet. Med.* 188, 105280. <http://dx.doi.org/10.1016/j.prevetmed.2021.105280>.
- Büttner, K., Krieter, J., Traulsen, A., Traulsen, I., 2013. Static network analysis of a pork supply chain in Northern Germany—Characterisation of the potential spread of infectious diseases via animal movements. *Prev. Vet. Med.* 110, 418–428. <http://dx.doi.org/10.1016/j.prevetmed.2013.01.008>.
- Candeloro, L., Savini, L., Conte, A., 2016. A new weighted degree centrality measure: The application in an animal disease epidemic. *PLoS One* 11, e0165781. <http://dx.doi.org/10.1371/journal.pone.0165781>.
- Chin, W.C.B., Bouffanais, R., 2020. Spatial super-spreaders and super-susceptibles in human movement networks. *Sci. Rep.* 10 (1), 18642. <http://dx.doi.org/10.1038/s41598-020-75697-z>.
- Colman, E., Holme, P., Sayama, H., Gershenson, C., 2019. Efficient sentinel surveillance strategies for preventing epidemics on networks. *PLoS Comput. Biol.* 15, e1007517. <http://dx.doi.org/10.1371/journal.pcbi.1007517>.
- Csárdi, G., Nepusz, T., Traag, V., Horvát, S., Zanini, F., Noom, D., Müller, K., 2024. igraph: Network analysis and visualization in R. <http://dx.doi.org/10.5281/zenodo.7682609>, URL <https://CRAN.R-project.org/package=igraph>. R package version 2.0.1.1.
- da Silva, R.A.P., Viana, M.P., da Fontoura Costa, L., 2012. Predicting epidemic outbreak from individual features of the spreaders. *J. Stat. Mech. Theory Exp.* 2012 (07), P07005. <http://dx.doi.org/10.1088/1742-5468/2012/07/P07005>.
- Dorman, M., 2023. Nngeo: k-nearest neighbor join for spatial data. URL <https://CRAN.R-project.org/package=nngoe>. R package version 0.4.7.
- Dubé, C., Ribble, C., Kelton, D., McNab, B., 2009. A review of network analysis terminology and its application to foot-and-mouth disease modelling and policy development. *Transbound. Emerg. Dis.* 56 (3), 73–85. <http://dx.doi.org/10.1111/j.1865-1682.2008.01064.x>.
- Enright, J., Kao, R.R., 2018. Epidemics on dynamic networks. *Epidemics* 24, 88–97. <http://dx.doi.org/10.1016/j.epidem.2018.04.003>.
- European Parliament and The Council, 2016. Regulation (EU) 2016/429. <https://eur-lex.europa.eu/eli/reg/2016/429/oj>.
- Freeman, L.C., 1978. Centrality in social networks conceptual clarification. *Soc. Netw.* 1, 215–239. [http://dx.doi.org/10.1016/0378-8733\(78\)90021-7](http://dx.doi.org/10.1016/0378-8733(78)90021-7).
- Ghanem, M., Magnien, C., Tarissan, F., 2019. Centrality metrics in dynamic networks: A comparison study. *IEEE Trans. Netw. Sci. Eng.* 6, 940–951. <http://dx.doi.org/10.1109/TNSE.2018.2880344>.
- Granovetter, M.S., 1973. The strength of weak ties. *Am. J. Sociol.* 78, 1360–1380. <http://dx.doi.org/10.1086/225469>.
- Holme, P., 2005. Network reachability of real-world contact sequences. *Phys. Rev. E* 71, 046119. <http://dx.doi.org/10.1103/PhysRevE.71.046119>.
- Hopcroft, J., Khan, O., Kulis, B., Selman, B., 2004. Tracking evolving communities in large linked networks. *Proc. Natl. Acad. Sci.* 101, 5249–5253. <http://dx.doi.org/10.1073/pnas.0307750100>.
- Jolly, A., 2001. Sexual networks and sexually transmitted infections: A tale of two cities. *J. Urban Heal.* Bull. N. Y. Acad. Med. 78, 433–445. <http://dx.doi.org/10.1093/jurban/78.3.433>.
- Kamp, C., Moslonka-Lefebvre, M., Alizon, S., 2013. Epidemic spread on weighted networks. *PLoS Comput. Biol.* 9, e1003352. <http://dx.doi.org/10.1371/journal.pcbi.1003352>.
- Keeling, M.J., Rohani, P., 2011. *Modeling Infectious Diseases in Humans and Animals*. Princeton University Press, New Jersey, pp. 15–53. <http://dx.doi.org/10.2307/j.ctvc4gk0.5>.
- Kharchenko, P., Petukhov, V., Biederstedt, E., 2022. leidenAlg: Implements the Leiden algorithm via an R interface. URL <https://CRAN.R-project.org/package=leidenAlg>. R package version 1.0.5.
- Kim, H., Anderson, R., 2012. Temporal node centrality in complex networks. *Phys. Rev. E* 85, 026107. <http://dx.doi.org/10.1103/PhysRevE.85.026107>.
- Kitsak, M., Gallos, L.K., Havlin, S., Liljeros, F., Muchnik, L., Stanley, H.E., Makse, H.A., 2010. Identification of influential spreaders in complex networks. *Nat. Phys.* 6 (11), 888–893. <http://dx.doi.org/10.1038/nphys1746>.
- Lentz, H.H., Koher, A., Hövel, P., Gethmann, J., Sauter-Louis, C., Selhorst, T., Conraths, F.J., 2016. Disease spread through animal movements: A static and temporal network analysis of pig trade in Germany. *PLoS One* 11, e0155196. <http://dx.doi.org/10.1371/JOURNAL.PONE.0155196>, URL <https://journals.plos.org/plosone/article?id=10.1371/journal.pone.0155196>.
- Lockhart, A.B., Thrall, P.H., Antonovics, J., 1996. Sexually transmitted diseases in animals: Ecological and evolutionary implications. *Biol. Rev.* 71, 415–471. <http://dx.doi.org/10.1111/j.1469-185X.1996.tb01281.x>.
- Lysholm, S., Chatters, G.L., Bari, C.D., Hughes, E.C., Huntington, B., Rushton, J., Thomas, L., 2025. A framework for quantifying the multisectoral burden of animal disease to support decision making. *Front. Vet. Sci.* 12, <http://dx.doi.org/10.3389/fvets.2025.1476505>.
- Marchiori, M., Latora, V., 2000. Harmony in the small-world. *Phys. A* 285, 539–546. [http://dx.doi.org/10.1016/S0378-4371\(00\)00311-3](http://dx.doi.org/10.1016/S0378-4371(00)00311-3).
- Mcassey, M.P., Bijma, F., 2015. A clustering coefficient for complete weighted networks. *Netw. Sci.* 3, 183–195. <http://dx.doi.org/10.1017/nws.2014.26>.
- McCallum, H., 2001. How should pathogen transmission be modelled? *Trends Ecol. Evolut.* 16, 295–300. [http://dx.doi.org/10.1016/S0169-5347\(01\)02144-9](http://dx.doi.org/10.1016/S0169-5347(01)02144-9).
- Natale, F., Giovannini, A., Savini, L., Palma, D., Possenti, L., Fiore, G., Calistri, P., 2009. Network analysis of Italian cattle trade patterns and evaluation of risks for potential disease spread. *Prev. Vet. Med.* 92, 341–350. <http://dx.doi.org/10.1016/j.prevetmed.2009.08.026>.
- Newman, M.E.J., 2001. Scientific collaboration networks. II. Shortest paths, weighted networks, and centrality. *Phys. Rev. E* 64 (1), 016132. <http://dx.doi.org/10.1103/PhysRevE.64.016132>, URL <https://link.aps.org/doi/10.1103/PhysRevE.64.016132>.
- Newman, M., 2004. Analysis of weighted networks. *Phys. Rev. E* 70, 056131. <http://dx.doi.org/10.1103/PhysRevE.70.056131>.
- Newman, M., 2018. *Networks*, vol. 1, Oxford University Press, Oxford, <http://dx.doi.org/10.1093/oso/9780198805090.001.0001>.
- Nielsen, S.S., Alvarez, J., Bicot, D.J., Calistri, P., Canali, E., Depner, K., Drewe, J.A., Garin-Bastuji, B., Rojas, J.L.G., Gortázar, C., Herskin, M., Michel, V., Chueca, M.Á.M., Padalino, B., Pasquali, P., Roberts, H.C., Sihvonen, L.H., Spoolder, H., Ståhl, K., Velarde, A., Viltrop, A., Winckler, C., Gubbins, S., Libeau, G., Broglia, A., Aznar, I., der Stede, Y.V., 2021. Assessment of the control measures of the category a diseases of animal health law: peste des petits ruminants. *EFSA J.* 19, <http://dx.doi.org/10.2903/j.efsa.2021.6708>.
- Oettershagen, L., Mutzel, P., Kriege, N.M., 2022. Temporal walk centrality: Ranking nodes in evolving networks. In: *Proceedings of the ACM Web Conference 2022. WWW '22*, Association for Computing Machinery, New York, NY, USA, pp. 1640–1650. <http://dx.doi.org/10.1145/3485447.3512210>.
- O'Hara, K.C., Beltrán-Alcrudo, D., Hovari, M., Tabakovski, B., Martínez-López, B., 2022. Network analysis of live pig movements in North Macedonia: Pathways for disease spread. *Front. Vet. Sci.* 9, <http://dx.doi.org/10.3389/fvets.2022.922412>.
- Passafaro, T.L., Fernandes, A.F., Valente, B.D., Williams, N.H., Rosa, G.J., 2020. Network analysis of swine movements in a multi-site pig production system in Iowa, USA. *Prev. Vet. Med.* 174, 104856. <http://dx.doi.org/10.1016/J.PREVTMED.2019.104856>.
- Pebesma, E., 2018. Simple features for R: Standardized support for spatial vector data. *R J.* 10 (1), 439–446. <http://dx.doi.org/10.32614/RJ-2018-009>.
- Pérez-Ortiz, M., Manescu, P., Caccioli, F., Fernández-Reyes, D., Nachev, P., Shawe-Taylor, J., 2022. Network topological determinants of pathogen spread. *Sci. Rep.* 12, 7692. <http://dx.doi.org/10.1038/s41598-022-11786-5>.
- Puspitarani, G.A., Fuchs, R., Fuchs, K., Ladinig, A., Desvars-Larrive, A., 2023a. Network Analysis of Pig Movement Data as an Epidemiological Tool: an Austrian Case Study. <http://dx.doi.org/10.6084/m9.figshare.21904995.v1>, Software.
- Puspitarani, G.A., Fuchs, R., Fuchs, K., Ladinig, A., Desvars-Larrive, A., 2023b. Network analysis of pig movement data as an epidemiological tool: an Austrian case study. *Sci. Rep.* 13 (1), 9623. <http://dx.doi.org/10.1038/s41598-023-36596-1>.
- R. Core Team, 2021. *R: A Language and Environment for Statistical Computing*. R Foundation for Statistical Computing, Vienna, Austria, URL <https://www.R-project.org/>.
- Radicchi, F., Castellano, C., Cecconi, F., Loreto, V., Parisi, D., 2004. Defining and identifying communities in networks. *Proc. Natl. Acad. Sci.* 101 (9), 2658–2663. <http://dx.doi.org/10.1073/pnas.0400054101>, URL <https://www.pnas.org/doi/abs/10.1073/pnas.0400054101>.
- Rautureau, S., Dufour, B., Durand, B., 2011. Vulnerability of animal trade networks to the spread of infectious diseases: A methodological approach applied to evaluation and emergency control strategies in Cattle, France, 2005. *Transbound. Emerg. Dis.* 58, 110–120. <http://dx.doi.org/10.1111/j.1865-1682.2010.01187.x>.
- Rautureau, S., Dufour, B., Durand, B., 2012. Structural vulnerability of the French swine industry trade network to the spread of infectious diseases. *Animal* 6, 1152–1162. <http://dx.doi.org/10.1017/S175173111002631>.
- Robinson, S., Christley, R., 2007. Exploring the role of auction markets in cattle movements within Great Britain. *Prev. Vet. Med.* 81, 21–37. <http://dx.doi.org/10.1016/j.prevetmed.2007.04.011>.
- RStudio Team, 2020. *RStudio: Integrated Development Environment for R*. RStudio, PBC, Boston, MA, URL <http://www.rstudio.com/>.
- Schley, D., Whittle, S., Taylor, M., Kiss, I.Z., 2012. Models to capture the potential for disease transmission in domestic sheep flocks. *Prev. Vet. Med.* 106, 174–184. <http://dx.doi.org/10.1016/j.prevetmed.2012.01.023>.
- Statistics Austria, Statistics Austria. <https://www.statistik.at/en/>.
- Statistics Austria, 2024. *Austria. Figures. Data. Facts*. Statistic Austria, Vienna, URL [www.statistik.at](http://www.statistik.at).
- Statistik Austria, Gliederung Österreichs in Gemeinden - Dataset - data.gv.at. [https://www.data.gv.at/katalog/en/dataset/stat\\_gliederung-osterreichs-in-gemeinden14f53](https://www.data.gv.at/katalog/en/dataset/stat_gliederung-osterreichs-in-gemeinden14f53).

- Traag, V.A., Waltman, L., van Eck, N.J., 2019. From Louvain to Leiden: guaranteeing well-connected communities. *Sci. Rep.* 2019 9:1 9, 1–12. <http://dx.doi.org/10.1038/s41598-019-41695-z>, URL <https://www.nature.com/articles/s41598-019-41695-z>.
- Trostle, P., Corzo, C.A., Reich, B.J., Machado, G., 2022. A discrete-time survival model for porcine epidemic diarrhoea virus. *Transbound. Emerg. Dis.* 69, 3693–3703. <http://dx.doi.org/10.1111/tbed.14739>.
- Valente, T.W., Coronges, K., Lakon, C., Costenbader, E., 2008. How correlated are network centrality measures? *Connect. (Toronto Ont.)* 28, 16–26.
- Volkova, V., Howey, R., Savill, N., Woolhouse, M., 2010a. Potential for transmission of infections in networks of cattle farms. *Epidemics* 2, 116–122. <http://dx.doi.org/10.1016/j.epidem.2010.05.004>.
- Volkova, V.V., Howey, R., Savill, N.J., Woolhouse, M.E.J., 2010b. Sheep movement networks and the transmission of infectious diseases. *PLoS One* 5, e11185. <http://dx.doi.org/10.1371/journal.pone.0011185>.
- Wasserman, S., Faust, K., 1994. *Social Network Analysis*. Cambridge University Press, Cambridge, <http://dx.doi.org/10.1017/CBO9780511815478>, URL <https://www.cambridge.org/core/product/identifier/9780511815478/type/book>.
- Weil, W. (Ed.), 2007. *Spatial point processes and their applications*. In: *Stochastic Geometry: Lectures Given at the C.I.M.E. Summer School Held in Martina Franca, Italy, September 13–18, 2004*, Springer Berlin Heidelberg, Berlin, Heidelberg, pp. 1–75. [http://dx.doi.org/10.1007/978-3-540-38175-4\\_1](http://dx.doi.org/10.1007/978-3-540-38175-4_1).
- West, D.B., et al., 2001. *Introduction to graph theory*, vol. 2, Prentice hall Upper Saddle River, New York.
- Wiratsudakul, A., Wongnak, P., Thanapongtharm, W., 2022. Emerging infectious diseases may spread across pig trade networks in Thailand once introduced: a network analysis approach. *Trop. Anim. Heal. Prod.* 54, 209. <http://dx.doi.org/10.1007/s11250-022-03205-8>.